

Corrosion of Stainless Steel in Simulated Tide of Fresh Natural Seawater of South East Pacific

Diego A. Fischer^{1,2}, Leslie Daille^{2,3}, Javiera Aguirre^{2,4}, Carlos Galarce^{1,2}, Francisco Armijo^{2,5}, Rodrigo De la Iglesia^{2,3}, Gonzalo Pizarro^{1,2}, Ignacio Vargas^{1,2}, Magdalena Walczak^{2,4,*}

¹ Departamento de Ingeniería Hidráulica y Ambiental, Escuela de Ingeniería, Pontificia Universidad Católica de Chile, Vicuña Mackenna 4860, Macul, Santiago, Chile.

² Marine Energy Research & Innovation Center (MERIC), Avda. Apoquindo 2827, Santiago, Chile.

³ Departamento de Genética Molecular y Microbiología, Facultad de Ciencias Biológicas, Pontificia Universidad Católica de Chile, Avda. Libertador Bernardo O'Higgins 340, Santiago, Chile

⁴ Departamento de Ingeniería Mecánica y Metalúrgica, Escuela de Ingeniería, Pontificia Universidad Católica de Chile, Vicuña Mackenna 4860, Macul, Santiago, Chile.

⁵ Laboratorio de Bioelectroquímica, Departamento de Química Inorgánica, Facultad de Química, Pontificia Universidad Católica de Chile Vicuña Mackenna 4860, 7820436, Macul, Santiago, Chile.

*E-mail: mwalczak@ing.puc.cl

Received: 4 May 2016 / Accepted: 7 June 2016 / Published: 7 July 2016

Whereas the initiation and advance of localized corrosion often limits a prolonged application of stainless steel in seawater, the particular conditions that trigger this type of corrosion are not fully understood due to high variability of water parameters and diversity of the biological component. In this study, coupons of AISI 304 and 316L were tested in fresh natural seawater of South East Pacific (coast of central Chile) employing two flow-through exposition racks: one keeping the coupons at full immersion and one allowing the simulation of tides through variable level of water effecting dry-wet cycles. Loss of weight and electrochemical characterization after 1, 5, 15 and 30 weeks of exposition revealed that for both materials the intermittent immersion results in considerably less corrosion, both general and localized. After 15 weeks, all samples showed a negative shift of OCP, i.e. the opposite of ennoblement, which is explained by the activity of microorganisms associated with change of season.

Keywords: marine corrosion, stainless steel, natural seawater, simulated tide, Pacific Ocean

1. INTRODUCTION

From the perspective of materials engineering, seawater is a medium that compromises functionality of most materials by weakening structures and components of machines exposed to it

through the processes of corrosion. With time, the structure or machine becomes unreliable and eventually ceases functioning. Hence, predicting the effect of seawater over materials in a long run is important to any structure designed to work in contact with seawater; these include off-shore oil and gas stations, docks, bridges, wharfs, pipelines as well as equipment processing seawater [1].

The specific damage experienced by the material as well as kinetics of its progression depends not only on the type of material but also on the mode of exposition to seawater, which might be fully immersed, partially immersed or intermittent. The most severe damage is typically found in the splash zone, where the spray of seawater is repeatedly spread over the material, wetting a surface otherwise exposed to the marine atmosphere [2,3]. Early studies have also shown that electrically isolated coupons, exposed at various relative heights with respect to the mean tide, concentrate most damage in the middle of the tidal zone. In continuous steel strips and electrically connected coupons the most severe damage was observed in the zone above mean-tide level, associated with the effect of splash [4-6]. A common explanation to this phenomenon is the differential aeration associated with higher oxygen content at the very surface of seawater producing galvanic action between the different locations at the same strip. The differential aeration has been shown to be associated with differential distribution of electrochemical potential and also differences in the composition of the resulting corrosion products [7].

Another key aspect of natural seawater relevant to corrosion is the presence of microorganisms, which colonize and grow on metallic surfaces producing non-uniform and variable biofilms that interfere with the native electrochemical processes. Microorganisms normally accelerate corrosion of metals, although the opposite, i.e. corrosion inhibition, might also take place, e.g. [8,9]. In case of stainless steels, the most common observation is that the presence of a biofilm is associated with a shift in open circuit potential (OCP) from its native (initial) value towards positive values; a process often referred to as ennoblement [10]. When OCP approaches the value of pitting potential the probability of developing localized corrosion increases dramatically.

One of the mechanisms proposed for explaining ennoblement is that of increased cathodic current [11]; however, the process or processes that produce the this enhancement are not fully explained. Dickinson *et al.* [12] have suggested that the effect is produced by manganese-depositing bacteria. The manganese oxides deposited over the steel surface would act as a permanent cathode increasing the intensity of the cathodic reaction; however the potential increase could not be related to the number of manganese-depositing bacteria [11]. Another possibility is that lowering of pH associated with bacterial activity, typically taking place under the biofilm, would promote the hydrogen evolution but the lower pH alone is insufficient for explaining the effect [13]. Other studies have suggested that ennoblement might be associated with the production of biopolymer metal complexes that increase the rate of oxygen reduction [14]. It is also possible that microorganisms interfere with the rate-determining step of the electrochemical reaction chain; for instance by accelerating the rate of H_2O_2 production [13]. Further studies have shown that the extent of ennoblement is determined by geographical location of the exposition site [15], which might be explained by the variable contribution of particular microorganisms to the OCP shift [16], which, in turn, is determined by the environmental conditions [17]. Also, interactions between microorganisms can further modulate the effect of biofilm over the process of corrosion [18].

Although a negative shift in the OCP is much less common it can also occur in association with the presence of microorganisms [19]. This opposite effect can also be explained by biofilm activity if appearance and disappearance of particular species associated with modification of environmental conditions are taken into account. The same author also suggests that the negative shift in OCP might produce crevices.

Due to the high number of parameters controlling the corrosion process in natural seawater, there are few standardized methods of testing. In particular, temperature, flow velocity, pH, amount of dissolved oxygen, salinity, presence of pollution, as well as microbial activity vary from location to location and also in time, making difficult the projection of corrosion mechanisms and the rate of material deterioration [20]. Most of the testing procedures proposed so far point at relative materials performance or verify the performance of a particular material at conditions defined a priori. For instance, Jeffrey and Melchers [3] tested the effect of vertical length of mild steel by attaching them with nylon bolts and washers to non-metallic support strips and those attached to a wooden jetty. Farro *et al.* [2] used a larger PVC structure with metal coupons attached to it, to study the effect of different tide zones on copper corrosion. The European Federation of Corrosion (EFC) supervised a corrosion study of several stainless steel grades using tanks of 200-300 L with continuous flow of fresh seawater in different geographical locations in Europe. The study was conducted with the purpose of verifying how the different conditions associated with the distinct locations may affect the corrosion process [10].

Although the above described approaches may provide the most resemblance to the natural environment, interpretation of the data is difficult because there are several parameters that cannot be controlled. The risk of losing samples due to storm surge is also a problem. Therefore, systems with control over the relevant corrosion parameters have also been explored. For instance, Mu *et al.* [21] studied the effect of simulated tide on mild steel by using tanks filled and emptied by pumps; however, this experiment employed artificial seawater and no microorganisms, hence it was not fully representing the natural condition. Corroborating the methodology for studying corrosion in marine water, there is no ideal solution and a trade-off between reproducing the natural conditions of exposition and control over these conditions is necessary in order to understand the underlying corrosion mechanisms [20].

In this work, we present a method for studying corrosion of stainless steel in fresh natural seawater at controlled conditions of exposition, permitting discrimination between continuous and intermitted immersion. Because South East Pacific at the coast of Chile is a poorly studied location for corrosion performance of materials, the alloys chosen for this study are the two most common stainless steels: AISI 304 and AISI 316L.

2. MATERIALS AND METHODS

2.1 Sample preparation

The materials used in this study are two commercial stainless steels differing in nominal content of main alloying elements: AISI 304 (X5CrNi189, material number 1.4301) and AISI 316L

(X2CrNiMo17-12-2, material number 1.4404). Cold rolled steel sheet of 3 mm thickness was cut into coupons of 100×20 mm using a slow cutting diamond blade so that the rolling direction corresponds with the longest dimension of the coupon. At the shortest edge two holes were drilled to enable mounting the sample in the exposition racks by the means of cable ties. Prior exposition each coupon was polished using emery paper (grit 240), rinsed with distilled water, degreased with acetone and finally dried by blowing hot air. For each sample retrieval, six duplicates were used.

2.2 Experimental set-up

The exposition experiments were conducted using natural fresh seawater in the facilities of the Estación Costera de Investigaciones Marinas (ECIM) of the Pontificia Universidad Católica de Chile, located at Pacific Ocean, 33°30'16"S; 71°38'23"O. The water quality parameters were measured using a HQ40d multi meter (HACH Company, Loveland, CO) and are described on Table 1.

Table 1. Water quality parameters at the beginning and the end of the experiment.

Time	1 Week	30 Weeks
pH	8.1	7.8
Conductivity (mS/cm)	54	57
O ₂ (mg/l)	9.8	7.4
Temperature (°C)	12.5	17

Two types of experimental set-up were used, one simulating continuous exposition under full immersion and one simulating the effect of tide. The first system, hereafter referred to as continuous flow system (CFS), consisted in acrylic racks of 53×29×16.5 cm, through which a constant flow of natural seawater was established. The homogeneity of the flow was assured by introducing a barrier with a pattern of holes as shown in Fig. 1A. The second system, hereafter referred to as simulated tide system (STS), consisted of a tank of 258×62×53 cm which was filled and emptied twice a day with natural seawater as seen on (Fig. 1B). The hourly schedule water level in the tank is shown in Fig. 1C. Both systems were operated in an opened mode, i.e. fed with seawater pumped directly from the Pacific Ocean. After flowing through the racks, the water was returned to the ocean at a slightly different location. Samples were retrieved for analysis after the following exposition times: 1 day, 1 week, 5 weeks, 15 weeks and finally 30 weeks.

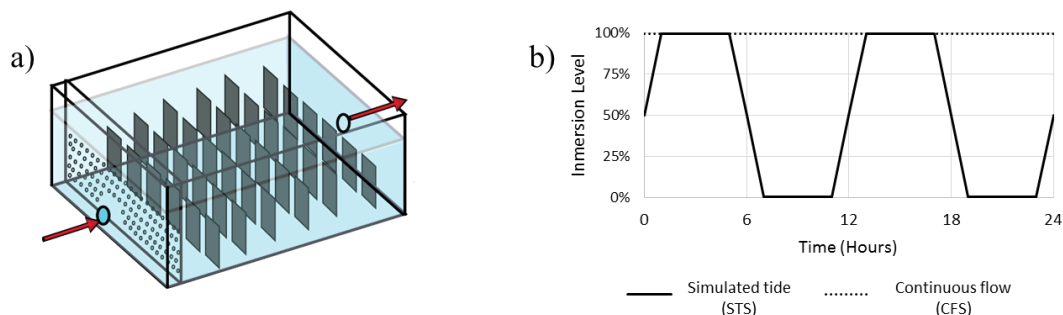


Figure 1. Structure and function of the exposition system: a) schematic view of the flow-through rack, b) position of water level in function of time; 100% - full immersion, 0% - samples entirely dry.

2.3 Sample characterization

Upon retrieval, the six-fold duplicate of each sample was visually inspected. Each sample was then cut off the sample holder without removing any of the possibly accumulated biomass and immediately transferred into a 50 ml Falcon tube filled with natural filtered seawater. Three duplicates were cleaned and weighted, and then visually inspected again to assess the corrosion damage at each side of the coupon. The remaining samples were used as follows: one for electrochemical characterization, one for electron microscope characterization, and one spared for complementary analysis.

Samples for microscopic examination were cut to the size of 10×15 mm using low speed diamond saw, and then fixed in a 2% solution of glutaraldehyde and stored at 4°C. Prior the microscopic observation each coupon was critical point dried and coated with a thin film of gold to render the surface conducting. Observations were completed using scanning electron microscope (SEM), LEO 1420VP (LEO Electron Microscopy Ltd., UK).

2.4 Corrosion testing

Visual appearance of each sample was evaluated and documented photographically immediately after retrieving from the exposition rack. Samples used for weight control (triplicate), after collecting from the exposition rack were sonicated in 50 mL of sterile water for 5 minutes (Elmasonic S 30H, Elma Schmidbauer GmbH, Alemania), washed using water and soap, degreased with acetone, and dried with hot air. Analytical balance was then used for determine the actual weight. Samples used for electrochemical analysis were carried to Santiago, Chile, in 50 ml falcon tubes filled with filtered (0.2 μm) fresh natural seawater. The electrochemical measurements were performed using CH-instrument 750-D in a conventional three electrode cell using Ag/AgCl as reference and a graphite rod as counter electrode. After determine open circuit potential (OCP), the polarization curve was measured starting at -0.5 V vs. OCP until the current density of 1 mA/cm² was reached, at the scanning rate of 0.005 V/s.

3. RESULTS

3.1 Visual inspection

In general, all samples collected after given exposition time for given exposition conditions were affected in a similar way and to a similar degree. After 1 week of exposition sparse corrosion products, distributed homogeneously were observed at the edges of the coupons. With increasing exposition time more corrosion products (red rust) appear at the sample surface, mostly close to and at the edges as well as at some of the surface irregularities. In general, for the same exposition time, the coupons exposed to the simulated tide appear to have accumulated less corrosion products as compared with the continuous flow exposition indicating to be less affected by corrosion.

After 30 weeks of exposition two of the AISI 304 samples in the continuous flow system produced crevices of considerable size at on the cut edge. An example of the crevice is shown in Figure 2.

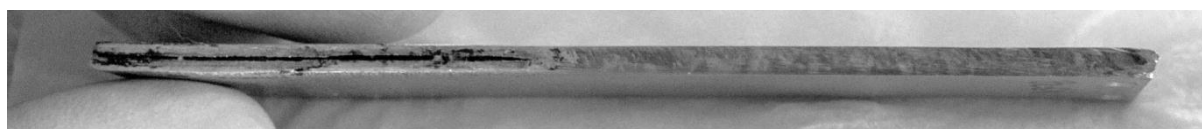


Figure 2. Visual appearance of the cut edge of AISI 304 after 30 weeks of exposition in the continuous flow system. The image has been digitally processed (adjustment of contrast) for better visualization of the crevice.

3.2 Microscopic characterization

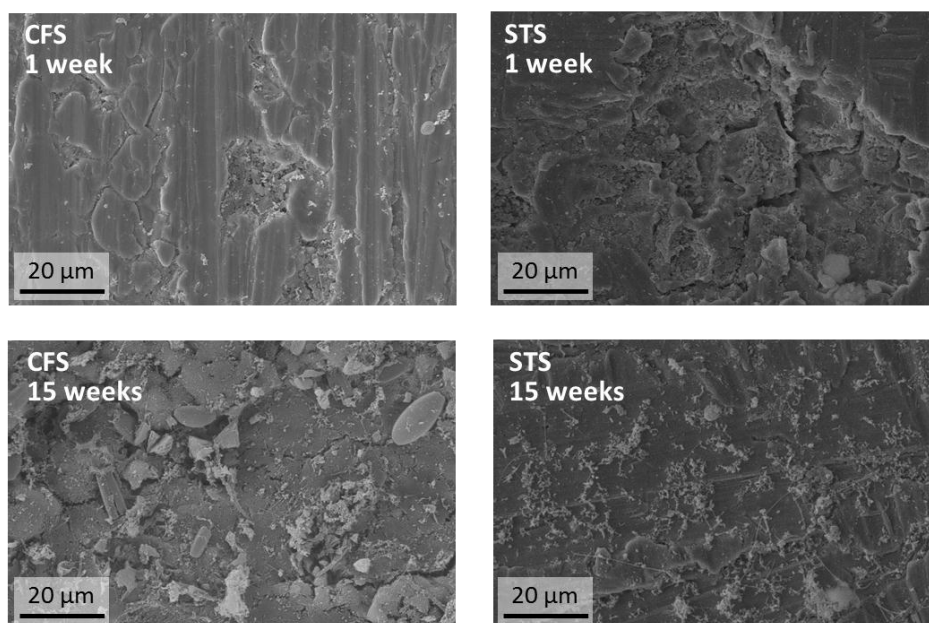


Figure 3. Representative SEM micrographs of AISI 304 after 1 and 15 weeks of exposition to fresh seawater in either continuous flow (CFS) or simulated tide (STS) system.

Figure 3 shows the SEM micrographs of AISI 304 retrieved after 1 week and 15 weeks, respectively, exposed at either of the systems. Analogous micrographs for the AISI 316L are shown in Figure 4. Initially, all samples were affected to a similar degree with the surface irregularities that may be attributed to the initial condition of the alloy plate. At prolonged exposition time, biomass has grown, including various types of bacteria and eukaryotes. In the case of CFS, the coupons were fully covered with bacteria and eukaryotes, whereas the biomass of coupons exposed in STS was formed mainly by bacteria and EPS (extracellular polymeric substances).

AISI 304 and 316L samples looked similar to their respective analogues along the experiment; however, there seems to be less biomass growing on the surface of AISI 316L as compared with AISI 304. This is especially true in the case of CFS.

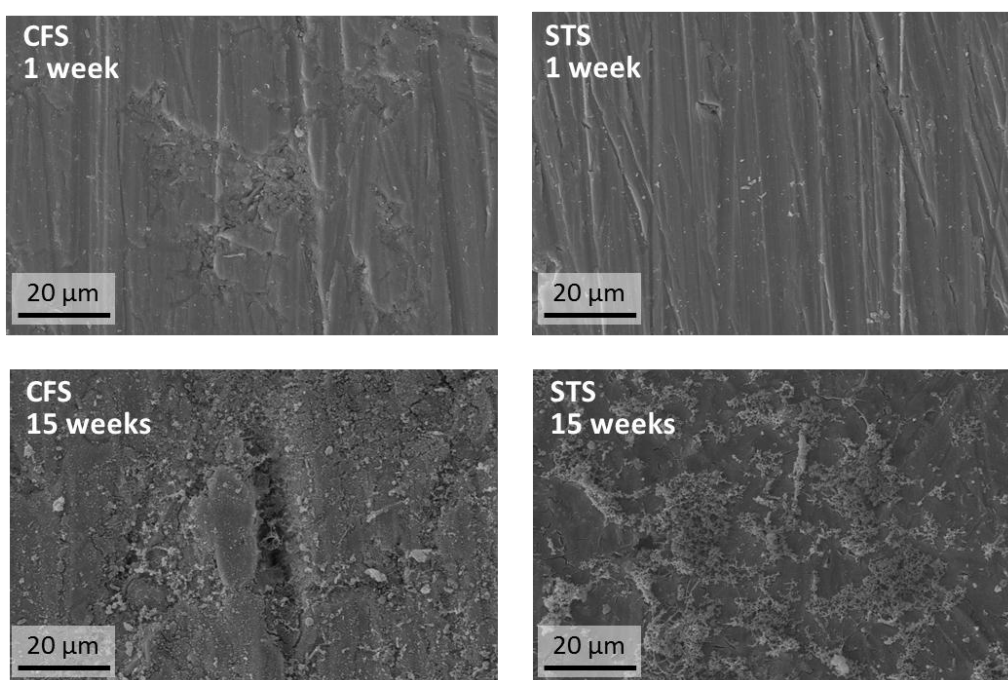


Figure 4. Representative SEM micrographs of AISI 316L after 1 and 15 weeks of exposure to fresh seawater in either continuous flow (CFS) or simulated tide (STS) system.

3.3 Weight loss

Table 3 shows the mass loss registered along the experiment. CFS samples suffered mass loss around two orders of magnitude higher than the STS samples on both metals. Differences in mass loss are produced mainly by the system instead of the alloy, although the average mass loss of AISI 304 is higher than AISI 316L samples. The CFS mass loss had a large variability on every sampling week on both metals, and on every set of triplicates one out of the samples had almost zero mass loss. On STS samples variability was low possibly because mass loss were too low and close to the limit of detection of the analytical balance.

Table 2. Weight loss expressed in mpy.

Exposition	AISI 304		AISI 316L	
	CFS	STS	CFS	STS
1 Week	-0.025 ± 0.014	-0.024 ± 0.009	-0.004 ± 0.017	-0.044 ± 0.055
5 Weeks	-0.283 ± 0.400	-0.009 ± 0.016	-0.181 ± 0.146	-0.136 ± 0.163
15 Weeks	-0.766 ± 0.542	-0.012 ± 0.017	-0.567 ± 0.425	-0.021 ± 0.029
30 Weeks	-0.792 ± 0.735	-0.006 ± 0.003	-0.442 ± 0.132	0.000 ± 0.001

3.4 Electrochemical characterization

The evolution of OCP is shown in Figure 5. During the initial 5 weeks almost all samples have undergone ennoblement increasing their OCP by a variable percentage. This trend then reverted for AISI 304 exposed at continuous flow system and after 15 to 30 weeks all the samples decreased their OCP; in some cases even below the value registered at the beginning of the experiment.

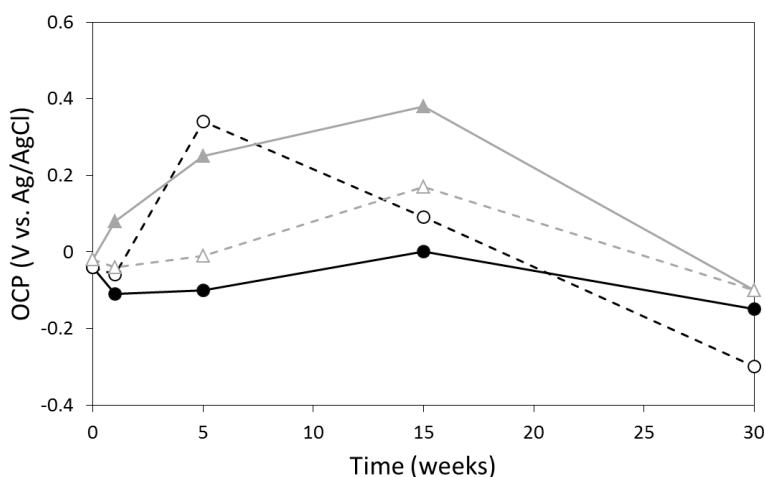


Figure 5. Open circuit potential registered in filtered fresh seawater for samples retrieved after different exposition times. Curve description: AISI 304 exposed in CFS (-○-), AISI 304 exposed in STS (-△-), AISI 316L exposed in CFS (-●-), AISI 316L exposed in STS (-▲-).

Figure 6 summarizes all the polarization curves measured on retrieved samples. For almost all samples the corrosion potential is different from the previously measured open circuit potential suggesting the sample surface was modified during cathodic polarization. On the other hand, pitting potential was only observed after first week of exposition. And its value is slightly higher on the AISI 316L samples (around 0.6 V) as compared with AISI 304 (around 0.54 V), suggesting the increased pitting resistance of AISI 316L. After longer exposition times, no current increase that could be associated with pitting is observed at the anodic branch of the polarization curves.

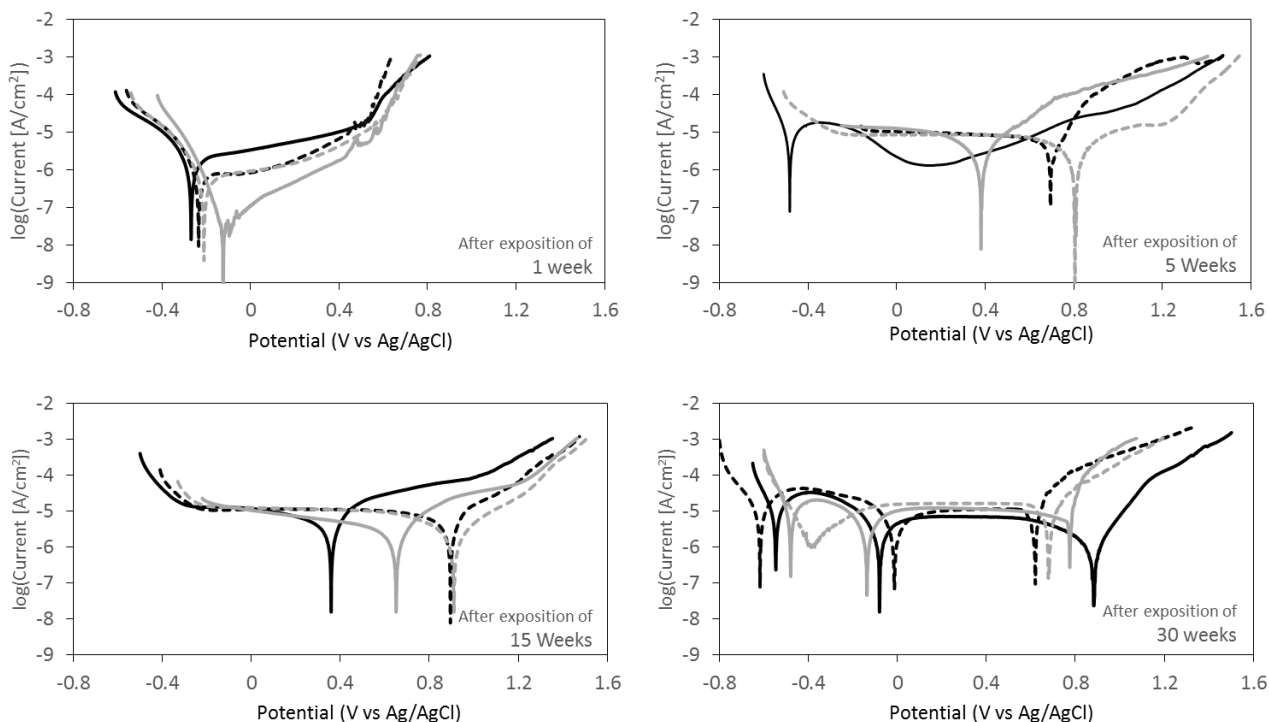


Figure 6. Polarization curves registered in filtered fresh seawater after exposition. Curve description: AISI 304 exposed in CFS (———), AISI 304 exposed in STS (- - - - -), AISI 316L exposed in CFS (———), AISI 316L exposed in STS (- - - - -)..

Notably, all samples retrieved after 30 weeks produced polarization curves with multiple equilibrium potentials. With the exception of AISI 316L exposed in STS these were two equilibrium potentials while all other samples produced three. These multiple equilibria can be explained by the active-passive behavior of stainless steel as presented graphically in Figure 7 and explained with detail in section 4.

4. DISCUSSION

The weight loss of both stainless materials obtained in our experiment is consistent with results reported in literature for similar exposition times. In the case of CFS corrosion rate from weight loss after 210 days corresponds with 0.79 mpy and 0.44 mpy for the AISI 304 and AISI 316L, respectively. These values are between the low values found for Arabian Gulf sweater by Al-Fozan *et al.* [22] reporting after 199 days on fully submerged samples the equivalent of 0.014 mpy and 0.01 mpy for the AISI 304 and AISI 316L, respectively; and the high values found by Al-Muhanna *et al.* [23] reporting after 180 days of fully submerged samples also for Arabian Gulf, presumably different location, the equivalent of 1.2 mpy and 1.18 mpy for AISI 304 and AISI 316L, respectively. Weight losses reported for water quality similar to South East Pacific at Pint Mugu, California, by Reinhart and Jenkins [24] after 1 year of exposition amounted to around 0.63 mpy and 0.25 mpy for AISI 304 and AISI 316, respectively.

The lower mass losses obtained for samples exposed in the simulated tide system are two orders of magnitude lower than their analogues exposed in the continuous flow system. It might be related with the shorter effective time of submersion in water and thus shorter time of wetness. However, the magnitude of the difference can hardly be explained by this effect, especially that the tidal zone is normally associated with increased corrosion damage [2,3]. However, contrary to the natural tide, in our system the splash effect was not included in the exposition, hence the effective time of wetness is shorter than that in a real system. On the other hand, the longer exposition to air allows for consolidation of the passive layer. This could be expected because a slightly thicker native passive layer have been shown to growth on AISI 316L in air as compared with layers grown in water [25]. However, the effect of drying on the activity of the biofilm has to be also taken into account. The SEM micrographs showed that samples exposed in the STS developed less biomass that would remain attached to the surface. The lower amount of biomass in this case suggests less microbiologically influenced corrosion as compared with the samples exposed in the CFS. These differences show how the distinct exposition conditions can result in selection of the microorganisms growing on the metal surface. Nevertheless, to provide a full explanation, more research would be necessary to determine how exactly the selection of microorganisms is affected by the position of water line and how does it affect the corrosion process. Another explanation to the lower mass loss observed in the STS is that the coupons were not sufficiently long (vertical direction) to produce considerable galvanic effect associated with differential aeration. In longer samples, one end is always in contact with water permitting the buildup of a cathodic zone at the immersed surface and an anodic zone at the splash zone [26]. It is not the case in our system. Also, subsurface content of oxygen in our case can only be attributed to the equilibrium of oxygen dissolution with no mechanical enhancement by waving or other surface mixing.

The OCP results indicate ennoblement for all samples at early weeks followed by a shift towards negative values in the later weeks (Figure 5). This drop of OCP was possibly induced by the increase of water temperature associated with seasonal variation, around 5°C throughout the experiment (Table 1). Warmer water, containing less oxygen would produce less intensive cathodic current; however, the change in water temperature can also promote or inhibit growth of diverse microorganisms as suggested by Fera *et al.* [27] that possibly modify the value of OCP too.

The observed shift of OCP towards negative potential values is uncommon. The study by European Federation of Corrosion (EFC) conducted for multiple location has reported consistent increase of OCP for all the conditions [10]. Although, other less extensive studies with natural seawater, have shown that although ennoblement is the typical case, negative shifts in the corrosion potential might also occur, e.g. [28,29]. A possible explanation was provided by Yuan *et al.* [30,31] who showed that *Pseudomonas* NCIMB 2021 and *Desulfovibrio desulfuricans* in simulated seawater can produce a negative shift of OCP. They also proposed that this potential drop was accomplished through the detrimental action of the bacteria over the passive layer. Hence, it is possible that the seasonal variation of our exposition condition have induced the growth of a microorganism that resulted in negative shift of OCP.

On the other hand, negative shift in OCP seawaters might also be associated with the formation of crevices and the resulting depassivation of steel surface as suggested by the EFC's study [10]. In our

study, there were no intentional crevice formers included in the design of sample holding system, yet, two of the AISI 304 exposed in CFS have developed visible crevices at the cut-edge of respective coupons after 30 weeks (Figure 2). These defects might have resulted from OCP drop produced by the biofilms as suggested by Urquidi-Macdonald [19], possibly due to the season change. The OCP drop in such a case can be completed by enhancing the anodic current and/or by inhibiting the cathodic reaction [19]. The activity of the biofilm can produce differential aeration cells due to heterogeneity of oxygen consumption. Under such a modified zone, a local OCP drop may occur producing local active zones that in turn lead to the formation of crevices and the resulting material deterioration.

Polarization curves recorded after 30 weeks of exposition show multiple equilibrium potentials. These multiple potentials have been previously reported in literature, for instance for iron in alkaline solution [32]; however to our knowledge there is no such report for stainless steel in natural seawater. A possible explanation of this phenomenon is the interaction between multiple cathodic and anodic reactions, which can be visualized as intersection of cathodic and anodic branches of the polarization curve [33]. Figure 7 provides our explanation of the polarization curves reported in Figure 6, where anodic current of a passive metal is considered and the cathodic branches include hydrogen and oxygen half-reactions. For voltages higher than equilibrium of the oxygen reaction, anodic branch of the oxygen reaction is also taken into account. In this representation, each equilibrium potential corresponds with zero-sum of currents, a condition met at multiple potentials. It should be noted that this situation is only possible when the cathodic reaction of oxygen is slower than the anodic reaction of the metal in the range of potentials associated with the active zone of the metal (shoulder in the polarization curve). This circumstance might arise when low oxygen content, possibly localized, produces cathodic reaction of low slope. Another possibility is depassivation of the metallic surface, possibly localized, due to bacterial activity.

In the case of triple equilibria, the value of OCP recorded prior polarization is similar to the value of the middle equilibrium, i.e. intersection of the anodic shoulder of the metal reaction with the cathodic branch of the oxygen reaction near the Flade potential. In case of potential drop, the shifting OCP would imply higher anodic current and thus higher corrosion rates. This process may occur locally induced by the activity of the biofilm.

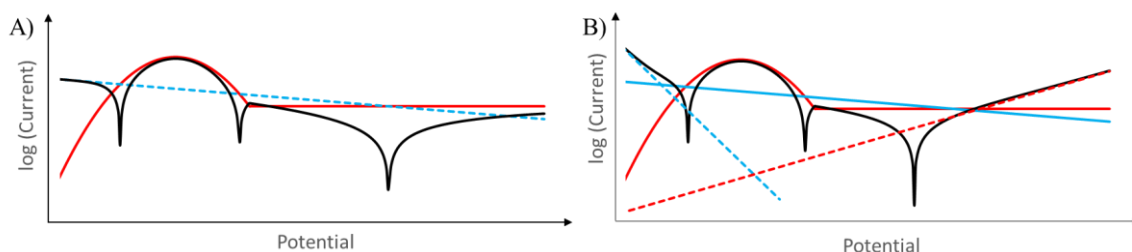


Figure 7. Schematic explanation of the shape of experimental polarization curves: A) Polarization curve with three equilibrium potentials and low current values at both cathodic and anodic extremes of the curve. B) Polarization curve with three equilibrium potentials and increase of current at both cathodic and anodic extremes of the curve. Curve description: total current (—), anodic branch of metal oxidation (—), anodic branch of oxygen reduction (---), cathodic branch oxygen reduction (—), cathodic branch of hydrogen reduction (---).

The crevices reported for AISI 304 after 30 weeks of exposure (Figure 2) can be explained by the drop of OCP [19]. Similar observations were reported by Melchers and Jeffrey [34] explaining that the vertical pattern could be associated with gravitational sliding of ferritic chloride down the sample, which would depassivate along the path [35]. Since AISI 304 has lower chromium content and no molybdenum alloyed it is more susceptible to such damage and therefore no crevice formation was observed for AISI 316L in which the potential drop was of larger value. The relative strength of the passive layer would also explain why there is no crevice formation in the STS exposure.

5. CONCLUSIONS

The analysis of AISI 304 and AISI 316L alloys exposed for 30 weeks to fresh natural seawater of South East Pacific at the coast of Chile allows for the following conclusions:

1. In both materials, an uncommon shift of open circuit potential toward cathodic values was observed and it is possibly related to seasonal changes of microorganisms' activity. This drop of potential might also be associated with the formation of lateral crevices.

2. Samples exposed in a simulated tide system, with the effect of splash excluded, experienced considerably less corrosion by weight loss, which was found to be associated with less pronounced evolution of biomass. This result might not be representative for a natural tide due to possible drying of biomass in the absence of aerosol or the lack of partial submersion preventing creation of differential aeration.

ACKNOWLEDGEMENTS

This research was funded by the Vicerrectoría de Investigación de la Pontificia Universidad Católica de Chile (PUC) through the project VRI-PUC N°01/2013. This study was conducted under the Marine Energy Research & Innovation Center (MERIC) project CORFO 14CEI2-28228. Special thanks to Charline Tessereau, Katherine Rojas and Francisca Rubio for laboratory assistant and sample preparation. In addition, Leslie Daille and Javiera Aguirre acknowledge CONICYT for their doctoral scholarships (beca N°21140415 and N°21150171, respectively).

References

1. R. E. Melchers, *Corros. Sci.*, 47 (2005) 2391.
2. N. W. Farro, L. Veleza, and P. Aguilar, *Open Corros. J.*, 2 (2009) 130.
3. R. Jeffrey and R. E. Melchers, *Corrosion*, 65 (2009) 695.
4. R. A. Humble, *Corrosion*, 4 (1948) 358.
5. F. L. La Que, *Am. Soc. Test. Mater.* (1951) .
6. C. P. Larrabee, *Corrosion*, 14 (1958) 21.
7. Y. Zou, J. Wang, Q. Bai, L. L. Zhang, X. Peng, and X. F. Kong, *Corros. Sci.*, 57 (2012) 202.
8. Z. Yu, J. Zhang, X. Zhao, X. Zhao, J. Duan, and X. Song, *Int. J. Electrochem. Sci.*, 9 (2014) 7587.
9. S. Liu, Y. Wang, D. Zhang, and Y. Wan, *Int. J. Electrochem. Sci.*, 8 (2013) 5330.
10. D. Feron, *Marine Corrosion of Stainless Steels*. Maney Publishing, London (2001)
11. B. J. Little and J. S. Lee, *Int. Mater. Rev.*, 59 (2014) 384.

12. W. H. Dickinson, F. Caccavo, B. Olesen, and Z. Lewandowski, *Appl. Environ. Microbiol.*, 63 (1997) 2502.
13. B. J. Little, J. S. Lee, and R. I. Ray, *Electrochim. Acta*, 54 (2008) 2.
14. S. C. Dexter and G. Y. Gao, *Corros. Sci.*, 44 (1988) 717.
15. M. S. and E. J. L. F. J. Martin, S. C. Dexter, "Relations between seawater ennoblement selectivity and passive film semiconductivity on Ni-Cr-Mo alloys," in *CORROSION/2007.*,
16. E. Kuş, R. Abboud, R. Popa, K. H. Nealson, and F. Mansfeld, *Corros. Sci.*, 47 (2005) 1063.,
17. Q. Zhang, P. Wang, and D. Zhang, *Int. J. Electrochem. Sci.*, 7 (2012) 11528.
18. J. J. Santana, F. J. Santana, J. E. Gonzalez, R. M. Souto, S. Gonzalez, and J. Morales, *Int. J. Electrochem. Sci.*, 7 (2012) 711.
19. D. D. M. M. Urquidi-Macdonald, "Modeling mechanisms in biocorrosion," in *Understanding Biocorrosion: Fundamentals and Applications*, Elsevier, (2014) 243.
20. F. Ijsseling, *Br. Corros. J.*, 24 (1989) 53.
21. X. Mu, J. Wei, J. Dong, and W. Ke, *J. Mater. Sci. Technol.*, 30 (2014) 1043.
22. S. a. Al-Fozan and A. U. Malik, *Desalination*, 228 (2008) 61.
23. K. Al-Muhanna, *Desalin. Water Treat.*, 29 (2011) 227.
24. Reinhart, Fred M., and James F. Jenkins. *Corrosion of materials in surface seawater after 12 and 18 months of exposure*. No. NCEL-TN-1213. NAVAL CIVIL ENGINEERING LAB PORT HUENEME CA, (1972).
25. S. Tardio, M.-L. Abel, R. Carr, J. E. Castle, and J. F. Watts, *J. Vac. Sci. Technol. A*, 33 (2015) 1.
26. R. Jeffrey and R. E. Melchers, *Corros. Sci.*, 51 (2009) 2291.
27. P. Fera, M. A. Siebel, W. G. Characklis, and D. Prieur, *Biofouling*, 1 (1989) 251.
28. A. Zaragoza-Ayala, N. Acuna, J. Aldana, and W. Solis, "Pitting Corrosion Behaviour of 316L Stainless Steel in Tropical SeaWater," in *CORROSION 96*, 1996, 504/2.
29. F. Mansfeld and B. Little, *Corrosion*, 45 (1989) 786.
30. S. J. Yuan, S. O. Pehkonen, Y. P. Ting, E. T. Kang, and K. G. Neoh, *Ind. Eng. Chem. Res.*, 47 (2008) 3008.
31. S. Yuan, B. Liang, Y. Zhao, and S. O. Pehkonen, *Corros. Sci.*, 74 (2013) 353.
32. Y. J. Li, Y. G. Wang, B. An, H. Xu, Y. Liu, L. C. Zhang, H. Y. Ma, and W. M. Wang, *PLoS One*, 11 (2016) e0146421.
33. R. G. Kelly, J. R. Scully, D. W. Shoesmith, and R. G. Buchheit, *Electrochemical Techniques in Corrosion Science and Engineering*, Maney Publishing, Inc (2003).
34. R. E. Melchers and R. Jeffrey, *Corrosion*, 64 (2008) 143.,
35. H. H. Uhlig, "Pitting in Stainless Steels and Other Passive Metals" in *Corrosion Handbook*, J. Wiley (1948) 165.